The Synchronization Ability of A Class of Multi-layer Coupled Networks

Jian Zhu, Tingting Xue*, Ping Pei, Xing Chen, Haiping Gao, Qian Liu

Abstract—**The synchronization of multi-layer networks have important theoretical and practical significance for the study of the interaction between multi-layer networks. Based on the multi-layer star-ring networks, this paper firstly defines a class of multi-layer wheel networks through graph theory. Secondly, using the master stability function model (MSF), the factors (such as coupling strength, number of layers, and number of nodes) that affect the synchronization ability of the multi-layer wheel networks are obtained under two different conditions of bounded and unbounded synchronized regions. Thirdly, simulation experiments are used to analyze how the above factors affect the synchronization ability. Finally, The structural parameter values of the multi-layer wheel networks to achieve the optimal synchronization ability are given, which provides a basis for controlling the synchronization ability.**

Index Terms—**multi-layer networks, the coupling strength, the wheel networks, simulation experiment, synchronization ability**

I. Introduction

THERE are many complex networks in nature, such as computer networks, power networks [1, 2], etc. Complex networks can be used as network models for systems such as neuroscience [3], control [4, 5], and disease detection [6]. As an important interdisciplinary subject, scholars from different disciplines carry out this research. In recent years, the research on complex networks have achieved many good results, such as synchronization [7-13], super-diffusion [14-16], network topology [17], node importance evaluation and containment control [18-19].

Mesh network is the most commonly used network form in Wan. Generally, there are two or more communication paths between any two node switches in the communication subnet. In this way, when one path fails, the information can also be sent through another path. In addition, the network can easily add new functions. As a kind of mesh network, the research on the synchronization ability of wheel network is very meaningful. The networks in the real world are not isolated, and the relationships between multi-layer networks cannot be determined by modeling single layer networks. In order to solve this problem, scholars proposed the supra-Laplacian matrix structure based on the diffusion dynamic equation of multi-layer networks, and analyzed the synchronization ability of the networks according to its eigenvalue spectrum [20]. Wei et al. studied the factors affecting the synchronization ability of two-layer regular networks, including star networks, ring networks and chain networks [21]. Wei et al. analyzed the synchronization ability of two-layer correlation networks and found that the inter-layer linking patterns and the coupling strength are the key factors to determine the synchronization ability [22]. Yang et al. derived the eigenvalue spectrum of two types of double layer hybrid directional weighted star-ring networks, and analyzed the relationships among the synchronization ability and network structure parameters [23]. The innovations of this article are as follows:

Firstly, we give the definitions of multi-layer wheel networks and introduce the basic knowledge of multi-layer networks synchronization.

Secondly, the supra-Laplacian spectrum of multi-layer coupled wheel networks are calculated, and the important indexes of synchronization ability are deduced in the case of different synchronized regions.

Thirdly, the relationships among the synchronization ability and parameters of multi-layer coupled wheel networks are analyzed.

Finally, the structural parameter values of the multi-layer wheel networks to achieve the optimal synchronization ability are given.

II. Preliminaries

A. Introduction of synchronization ability of multi-layer networks

In this article, the M-layer networks are considered and the number of single layer nodes is S. The network structure of each layer is the same. The corresponding nodes between layers are all connected, the dynamic equation of the ith node in the Nth layer can be described as [22]:

$$\dot{x}_i^N = f(x_i^N) + a\sum_{j=1}^{S}\omega_{ij}^N T(x_j^N) + d\sum_{V=1}^{M} d_i^{NV} K(x_i^N), \quad (1)$$

$$i = 1, 2, \cdots, S, N = 1, 2, \cdots, M.$$

Manuscript received December 10, 2021; revised November 1, 2022. This work was supported by the National Natural Science Foundation of China (no.61802316) and the National Science Foundation of Xinjiang (NSFXJ) (no.2021D01A65), the National Science Foundation of Xinjiang (NSFXJ) (no.2021D01B35), National innovation and entrepreneurship training program for College Students (no.202110994006), National innovation and entrepreneurship training program for College Students (no.202210994014).

Jian Zhu is a lecturer of School of Mathematics and Physic, Xinjiang Institute of Engineering, Urumqi, CO 830023 PR China (e-mail: zj17@xjie.edu.cn).

Tingting Xue is an associate professor of School of Mathematics and Physic, Xinjiang Institute of Engineering, Urumqi, CO 830023 PR China (phone: 0991-7977187; fax: 0991-7977187; e-mail: xuett@cumt.edu.cn).

Ping Pei is an associate professor of School of Mathematics and Physic, Xinjiang Institute of Engineering, Urumqi, CO 830023 PR China (e-mail: zl16@xjie.edu.cn).

Xing Chen is a professor of School of Mathematics and Physics, Xinjiang Institute of Engineering, Urumqi, CO 830023 PR China (e-mail: chenxingxjnu@163.com).

Haiping Gao is a lecturer of School of Basic Science, Xinjiang Institute of Light Industry Technology, Urumqi, CO 830021 PR China (e-mail: yqh@xjie.edu.cn).

Qian Liu is an undergraduate student of School of Information Engineering, Xinjiang Institute of Engineering, Urumqi, CO 830023 PR China (e-mail: xjgcxy104@163.com).

x_i^N is the state variable of the ith node in the Nth layer, $f(\times)$ is the dynamic function, a and d are the intralayer and interlayer coupling strengths, T and K are the intralayer and interlayer coupling functions.

$W^N = (\omega_{ij}^N) \in R^{S\times S}$ is the intra coupling matrix of the Nth layer, $\omega_{ii}^N = -\sum_{j=1,j\neq i}^{S}\omega_{ii}^N$, $\omega_{ij}^N = \begin{cases}1, & i\text{th node is connected with } j\text{th node}\\ 0, & \text{otherwise}\end{cases}$. $D_M = (d_i^{NV}) \in R^{M\times M}$ is the inter coupling matrix, $d_i^{NN} = -\sum_{V=1,V\neq N}^{M} d_i^{NV}$. Let i^N be ith node in Nth layer, i^V be ith node in Vth layer,

$$d_i^{NV} = \begin{cases}1, & i^N \text{ is connected with } i^V\\ 0, & \text{otherwise}\end{cases}.$$

Let Λ^N be the supra-Laplacian matrix of the intralayer in the Nth layer, Λ_{intra} be the supra-Laplacian matrix of the intralayer, $\Lambda^N = -aW^N \in R^{S\times S}$.

$$\Lambda_{intra} = \bigoplus_{N=1}^{M} W^N = \begin{pmatrix} W^1 & 0 & \cdots & 0\\ 0 & W^2 & \cdots & 0\\ \vdots & \vdots & \ddots & \vdots\\ 0 & 0 & \cdots & W^M \end{pmatrix} \quad (2)$$

Λ_{inter} denotes the supra-Laplacian matrix of the interlayer, $\Lambda_{inter} = -dD_M \otimes I_S$. $\bigotimes$ is Kronecker product, I_S is the identity matrix of $S\times S$. The supra-Laplacian matrix of multi-layer network is $\Lambda = \Lambda_{inter} + \Lambda_{intra}$.

Let the eigenvalues of the supra-Laplacian matrix Λ be $0 = \lambda_1 < \lambda_2 \leq \lambda_3 \leq \lambda_4 \leq \cdots \leq \lambda_{max}$. According to the MSF, the minimum nonzero eigenvalue of the supra-Laplacian matrix λ_2 is used to reflect the synchronization ability of multi-layer coupled networks in the unbounded synchronized region. The synchronization ability is positively correlated with λ_2. $r = \frac{\lambda_{max}}{\lambda_2}$ is used to reflect the synchronization ability of multi-layer coupled networks in the bounded synchronized region, the synchronization ability is negatively correlated with r [23].

B. The structure model of wheel networks

Let $G = (V(G), E(G))$ be a connected graph, where $V(G) = \{v_1, v_2, \cdots, v_{n-2}, v_{n-1}, v_n\}$ is the vertex set, $E(G) = \{(v_i, v_j)|i, j = 1, 2, 3, \cdots, n-1, n; i \neq j\}$ is the edge set. Let K_c be a complete graph with c nodes, P_k be a path with k vertices, and C_m be a cycle of length m.

In order to obtain the definition of multi-layer wheel networks, we introduce two graph operations as follows.

Definition 1 ([24]) G_1 denotes a simple graph with n^* vertices and m^* edges, G_2 denotes a simple graph with n^{**} vertices and m^{**} edges. $G_1 \circ G_2$ is obtained from one copy of G_1 and n_* copies of G_2 and then joining the ith vertex of G_1 to every vertex in the ith copy of $G_2 (i = 1, 2, 3, \cdots, n_*)$.

Definition 2 ([25]) G_1, G_2 represent two simple graphs, $G_1 \bigtriangledown G_2$ is obtained from the disjoint union of G_1 and G_2 by adding the edges $\{uv : u \in V(G_1), v \in V(G_2)\}$.

$G_c(c, m+1-c, k) = (K_c \bigtriangledown C_{m+1-c}) \circ P_k$, c is the number of central nodes, m is the length of cycle($m \geq c+2$), k is the number of nodes in path($k \geq 2$). An example of the single layer wheel network is shown Fig. 1. $G_c^M(c, m, k)$ are composed of M layers $G_c(c, m, k)$. A specific example is shown in Fig. 2.

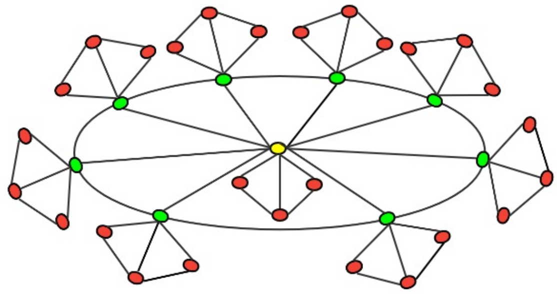

Fig. 1. Single layer wheel network $G_1(1, 8, 3)$.

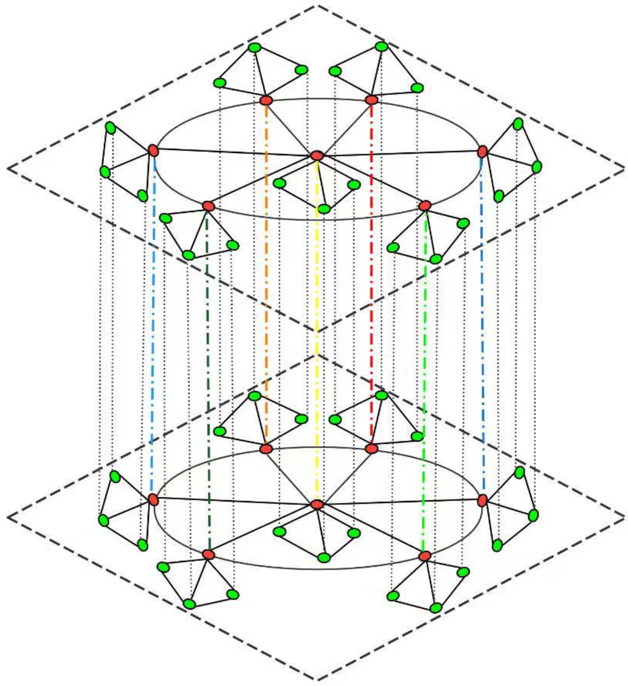

Fig. 2. Double layer wheel network $G_1^2(1, 6, 3)$.

III. The synchronization ability indexes of multi-layer wheel networks

A. The synchronization ability indexes of $G_1^M(1, m, k)$

According to the structure model of multi-layer wheel networks, we get the supra-Laplacian matrix of $G_1^M(1, m, k)$.

$$W_1 = \begin{pmatrix} 0 & 1 & 1 & \cdots & 1 & 1\\ 1 & -2 & 1 & \cdots & 0 & 0\\ 1 & 1 & -3 & \cdots & 0 & 0\\ \vdots & \vdots & \vdots & \ddots & \vdots & \vdots\\ 1 & 0 & 0 & \cdots & -3 & 1\\ 1 & 0 & 0 & \cdots & 1 & -2 \end{pmatrix}_{(k+1)\times(k+1)}$$

$$W_2 = \begin{pmatrix} 1 & 0 & 0 & \cdots & 0 & 0\\ 0 & 1 & 0 & \cdots & 0 & 0\\ 0 & 0 & 1 & \cdots & 0 & 0\\ \vdots & \vdots & \vdots & \ddots & \vdots & \vdots\\ 0 & 0 & 0 & \cdots & 1 & 0\\ 0 & 0 & 0 & \cdots & 0 & 1 \end{pmatrix}_{(m+1)\times(m+1)},$$

$$W_3=\begin{pmatrix}1&0&0&0&\cdots&0\\0&0&0&0&\cdots&0\\0&0&0&0&\cdots&0\\0&0&0&0&\cdots&0\\\vdots&\vdots&\vdots&\vdots&\ddots&\vdots\\0&0&0&0&\cdots&0\end{pmatrix}_{(k+1)\times(k+1)},$$

$$W_4=\begin{pmatrix}\Theta_1&1&1&\cdots&1\\1&\Theta_2&1&\cdots&1\\1&1&\Theta_2&\cdots&0\\\vdots&\vdots&\vdots&\ddots&\vdots\\1&1&0&\cdots&\Theta_2\end{pmatrix}_{(m+1)\times(m+1)},$$

where $\Theta_1=-k-m,\Theta_2=-k-3$.

The supra-Laplacian matrix of the intralayer in the Nth layer is

$$\Lambda_1^N=-aW_1\otimes W_2-aW_3\otimes W_4.$$

The supra-Laplacian matrix of $G_1^M(1,m,k)$ is

$$\Lambda_1=I_M\otimes\Theta_3+(I_M-J_M)\otimes(dI),\qquad(3)$$

where $\Theta_3=\Lambda_1^N+(M-1)dI$, J_M is the $M\times M$ matrix, whose entries are all 1.

The characteristic polynomial of matrix Λ_1 is

$$\Phi_I(\lambda)=det(\lambda I-\Lambda_1)=\begin{vmatrix}\Theta_4&dI&dI&\cdots&dI\\dI&\Theta_4&dI&\cdots&dI\\dI&dI&\Theta_4&\cdots&dI\\\vdots&\vdots&\vdots&\ddots&\vdots\\dI&dI&dI&\cdots&\Theta_4\end{vmatrix},$$

where $\Theta_4=\lambda I-\Lambda_1^N-(M-1)dI$.

From the properties of the determinant, we have

$$\Phi_I(\lambda)=|\lambda I-\Lambda_1^N||\lambda I-\Lambda_1^N-MdI|^{M-1}.(4)$$

The eigenvalue spectrum of Λ_1 is

$$0,(k+1)a,\frac{m+k+2\pm\sqrt{(m+k+2)^2-4(m+1)}}{2}a,$$

$$\underbrace{Md,(k+1)a+Md,}_{M-1}$$

$$\underbrace{\frac{m+k+2\pm\sqrt{(m+k+2)^2-4(m+1)}}{2}a+Md,}_{M-1}$$

$$\frac{e_\alpha\pm\sqrt{e_\alpha^2-4(e_\alpha-k-1)}}{2}a,$$

$$\underbrace{\frac{e_\alpha\pm\sqrt{(e_\alpha)^2-4(e_\alpha-k-1)}}{2}a+Md,}_{(M-1)}$$

$$(e_\alpha=4sin^2(\frac{\alpha\pi}{m})+k+2,\alpha=1,2,\cdots,m-1)$$

$$\underbrace{4asin^2(\frac{\beta\pi}{k})+a,}_{m+1}\underbrace{4asin^2(\frac{\beta\pi}{k})+a+Md}_{(M-1)(m+1)}.$$

$$(\beta=1,2,\cdots,k-1)$$

TABLE I

THE SYNCHRONIZATION ABILITY INDEXES OF $G_1^M(1,m,k)$.

		$m\uparrow$	$k\uparrow$	$a\uparrow$	$d\uparrow$	$M\uparrow$
λ_2	$\mu_1<Md$	$\downarrow$	$\downarrow$	$\uparrow$	$-$	$-$
	$\mu_1>Md$	$-$	$-$	$-$	$\uparrow$	$\uparrow$
r	$\mu_1<Md$	$\uparrow$	$\uparrow$	$\downarrow$	$\uparrow$	$\uparrow$
	$\mu_1>Md$	$\uparrow$	$\uparrow$	$\uparrow$	$\downarrow$	$\downarrow$

$\uparrow$ strengthen, $\downarrow$ weaken, $-$ unchange.

We get the minimum nonzero eigenvalue and the maximum eigenvalue as follows:

$$\lambda_2=min\{\mu_1,Md\},$$

$$\lambda_{max}=\frac{\omega_1+\sqrt{\omega_1^2-4(m+1)}}{2}a+Md,$$

where

$$\mu_1=\frac{e_1-\sqrt{e_1^2-4(e_1-k-1)}}{2}a,$$

$$e_1=4sin^2(\frac{\pi}{m})+k+2,\omega_1=m+k+2.$$

Then,

$$r=(\frac{\omega_1+\sqrt{(\omega_1)^2-4(m+1)}}{2}a+Md)/\lambda_2.$$

The specific relationships among the synchronization ability indexes and parameters are described in Table I.

B. The synchronization ability indexes of $G_2^M(2,m,k)$

Similar to section A, we get the supra-Laplacian matrix of $G_2^M(2,m,k)$,

$$W_5=\begin{pmatrix}\Theta_5&1&1&\cdots&1&1\\1&\Theta_5&1&\cdots&1&1\\1&1&\Theta_6&\cdots&0&1\\\vdots&\vdots&\vdots&\ddots&\vdots&\vdots\\1&1&0&\cdots&\Theta_6&1\\1&1&0&\cdots&1&\Theta_6\end{pmatrix}_{(m+1)\times(m+1)}$$

where $\Theta_5=-k-m,\Theta_6=-k-4$.

The supra-Laplacian matrix of the intralayer in the Nth layer is

$$\Lambda_2^N=-aW_1\otimes W_2-aW_3\otimes W_5.$$

The supra-Laplacian matrix of $G_2^M(2,m,k)$ is

$$\Lambda_2=I_M\otimes\Theta_7+(I_M-J_M)\otimes(dI),\qquad(5)$$

where $\Theta_7=\Lambda_2^N+(M-1)dI$.

The eigenvalue spectrum of Λ_2 is

$$0,(k+1)a,\underbrace{\frac{m+k+2\pm\sqrt{(m+k+2)^2-4(m+1)}}{2}a,}_{2}$$

TABLE II
THE SYNCHRONIZATION ABILITY INDEXES OF $G_2^M(2,m,k)$.

		$m\uparrow$	$k\uparrow$	$a\uparrow$	$d\uparrow$	$M\uparrow$
λ_2	$\mu_2 < Md$	$\downarrow$	$\downarrow$	$\uparrow$	$-$	$-$
	$\mu_2 > Md$	$-$	$-$	$-$	$\uparrow$	$\uparrow$
r	$\mu_2 < Md$	$\uparrow$	$\uparrow$	$\downarrow$	$\uparrow$	$\uparrow$
	$\mu_2 > Md$	$\uparrow$	$\uparrow$	$\uparrow$	$\downarrow$	$\downarrow$

$\uparrow$ strengthen, $\downarrow$ weaken, $-$ unchange.

$$\underbrace{Md, (k+1)a + Md,}_{M-1}$$

$$\underbrace{\frac{m+k+2 \pm \sqrt{(m+k+2)^2 - 4(m+1)}}{2} a + Md,}_{2(M-1)}$$

$$\frac{f_\alpha \pm \sqrt{f_\alpha^2 - 4(f_\alpha - k - 1)}}{2} a,$$

$$\underbrace{\frac{f_\alpha \pm \sqrt{(f_\alpha)^2 - 4(f_\alpha - k - 1)}}{2} a + Md,}_{(M-1)}$$

$$(f_\alpha = 4sin^2(\frac{\alpha\pi}{m-1}) + k + 3, \alpha = 1, 2, \cdots, m-2),$$

$$\underbrace{4asin^2(\frac{\beta\pi}{k}) + a,}_{m+1} \underbrace{4asin^2(\frac{\beta\pi}{k}) + a + Md}_{(M-1)(m+1)}.$$

$$(\beta = 1, 2, \cdots, k-1)$$

We get the minimum nonzero eigenvalue and the maximum eigenvalue as follows:

$$\lambda_2 = min\{\mu_2, Md\},$$

$$\lambda_{max} = \frac{\omega_1 + \sqrt{\omega_1^2 - 4(m+1)}}{2} a + Md,$$

where

$$\mu_2 = \frac{f_1 - \sqrt{f_1^2 - 4(f_1 - k - 1)}}{2} a,$$

$$f_1 = 4sin^2(\frac{\pi}{m-1}) + k + 3, \omega_1 = m + k + 2.$$

Then,

$$r = (\frac{\omega_1 + \sqrt{\omega_1^2 - 4(m+1)}}{2} a + Md)/\lambda_2.$$

The specific relationships among the synchronization ability indexes and parameters are described in Table II.

C. *The synchronization ability indexes of $G_c^M(c,m,k)$*

We use a similar method to study the synchronization ability indexes of multi-layer wheel networks with center nodes c.

The eigenvalue spectrum of $G_c^M(c,m,k)$ is derived as follows:

$$0, (k+1)a, \underbrace{\frac{m+k+2 \pm \sqrt{(m+k+2)^2 - 4(m+1)}}{2} a,}_{c}$$

$$\underbrace{Md, (k+1)a + Md,}_{M-1}$$

$$\underbrace{\frac{m+k+2 \pm \sqrt{(m+k+2)^2 - 4(m+1)}}{2} a + Md,}_{c(M-1)}$$

$$\frac{g_\alpha \pm \sqrt{g_\alpha^2 - 4(g_\alpha - k - 1)}}{2} a,$$

$$\underbrace{\frac{g_\alpha \pm \sqrt{g_\alpha^2 - 4(g_\alpha - k - 1)}}{2} a + Md,}_{(M-1)}$$

$$(g_\alpha = 4sin^2(\frac{\alpha\pi}{m+1-c}) + c + k + 1, \alpha = 1, 2, \cdots, m-c),$$

$$\underbrace{4asin^2(\frac{\beta\pi}{k}) + a,}_{m+1} \underbrace{4asin^2(\frac{\beta\pi}{k}) + a + Md}_{(M-1)(m+1)}.$$

$$(\beta = 1, 2, \cdots, k-1)$$

We get the minimum nonzero eigenvalue and the maximum eigenvalue as follows:

$$\lambda_2 = min\{\mu_3, Md\},$$

$$\lambda_{max} = \frac{\omega_1 + \sqrt{\omega_1^2 - 4(m+1)}}{2} a + Md,$$

where

$$\mu_3 = \frac{g_1 - \sqrt{g_1^2 - 4(g_1 - k - 1)}}{2} a,$$

$$g_1 = 4sin^2(\frac{\pi}{m+1-c}) + c + k + 1, \omega_1 = m + k + 2.$$

Then,

$$r = (\frac{\omega_1 + \sqrt{\omega_1^2 - 4(m+1)}}{2} a + Md)/\lambda_2.$$

The specific relationships among the synchronization ability indexes and parameters are described in Table III.

TABLE III
THE SYNCHRONIZATION ABILITY INDEXES OF $G_c^M(c,m,k)$.

		$m\uparrow$	$k\uparrow$	$a\uparrow$	$d\uparrow$	$M\uparrow$
λ_2	$\mu_3 < Md$	$\downarrow$	$\downarrow$	$\uparrow$	$-$	$-$
	$\mu_3 > Md$	$-$	$-$	$-$	$\uparrow$	$\uparrow$
r	$\mu_3 < Md$	$\uparrow$	$\uparrow$	$\downarrow$	$\uparrow$	$\uparrow$
	$\mu_3 > Md$	$\uparrow$	$\uparrow$	$\uparrow$	$\downarrow$	$\downarrow$

$\uparrow$ strengthen, $\downarrow$ weaken, $-$ unchange.

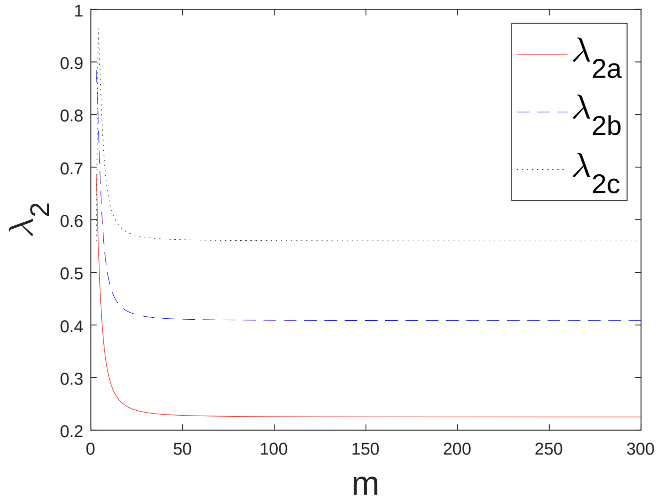

Fig. 3. The synchronization ability index changes with m

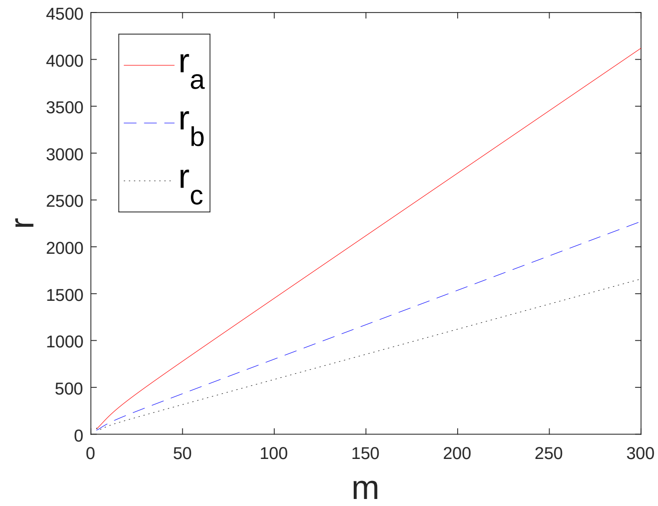

Fig. 4. The synchronization ability index changes with m

IV. NUMERICAL SIMULATION EXPERIMENT AND ANALYSIS

According to the relationships among the synchronization ability indexes and parameters in section III, the simulation experiments are carried out in the case of bounded and unbounded synchronized regions, and the variation of synchronization ability with each parameter are simulated. λ_{2a},

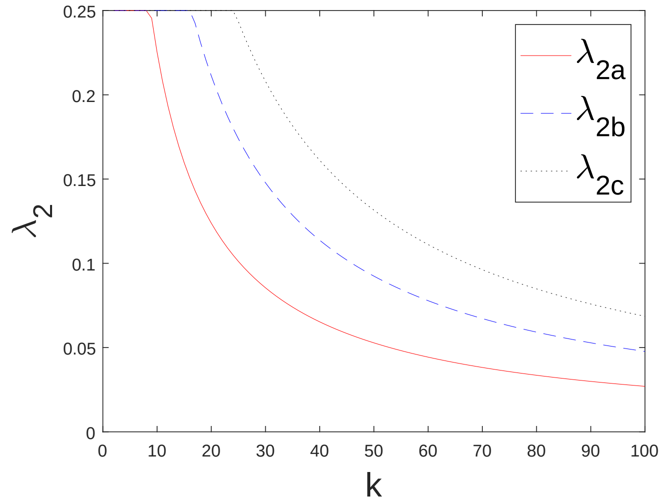

Fig. 5. The synchronization ability index changes with k

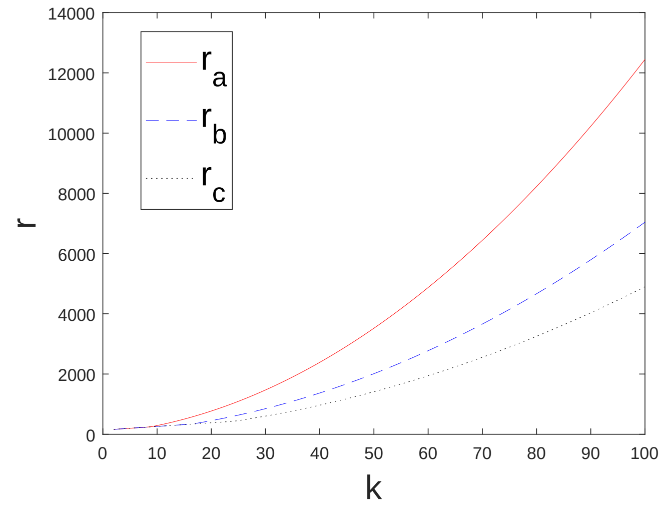

Fig. 6. The synchronization ability index changes with k

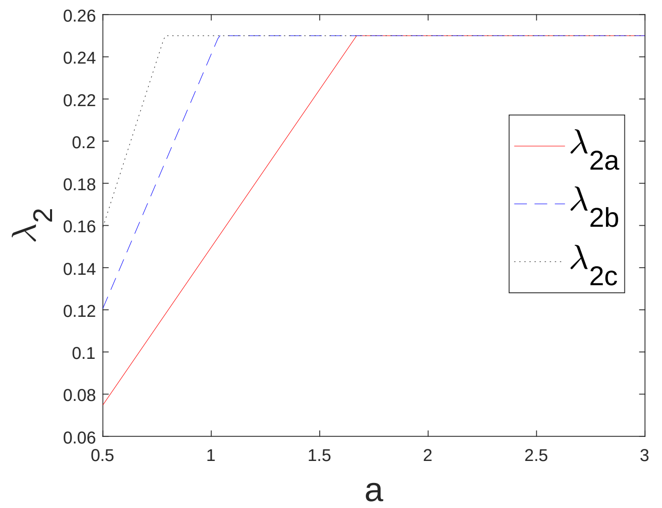

Fig. 7. The synchronization ability index changes with a

λ_{2b} and λ_{2c} represent the synchronization ability indexes of $G_c(c,m,k)(c=1,2,3)$ in the case of unbounded synchro-

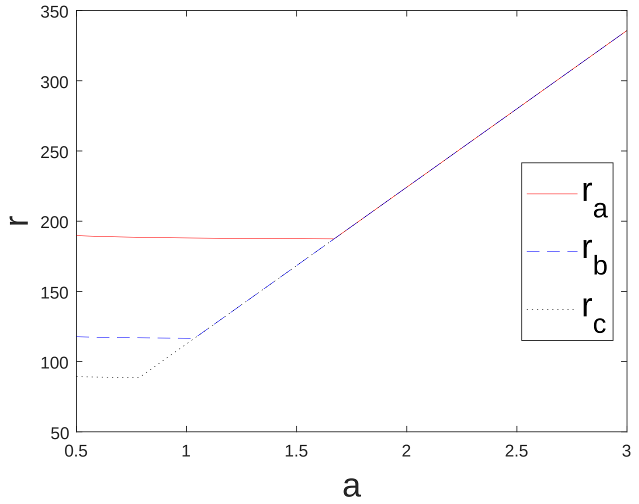

Fig. 8. The synchronization ability index changes with a

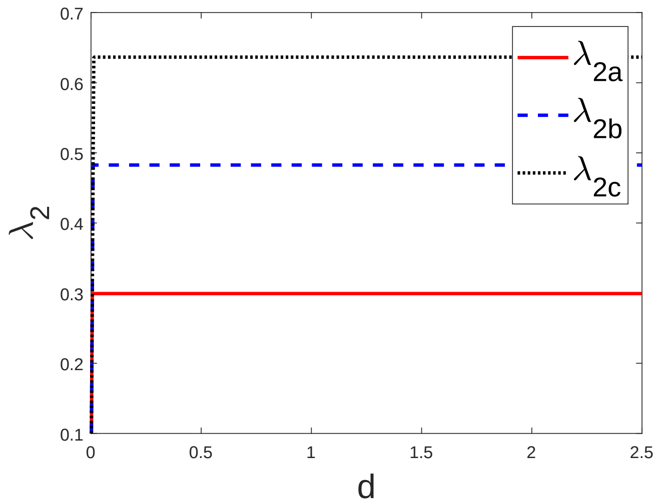

Fig. 9. The synchronization ability index changes with d

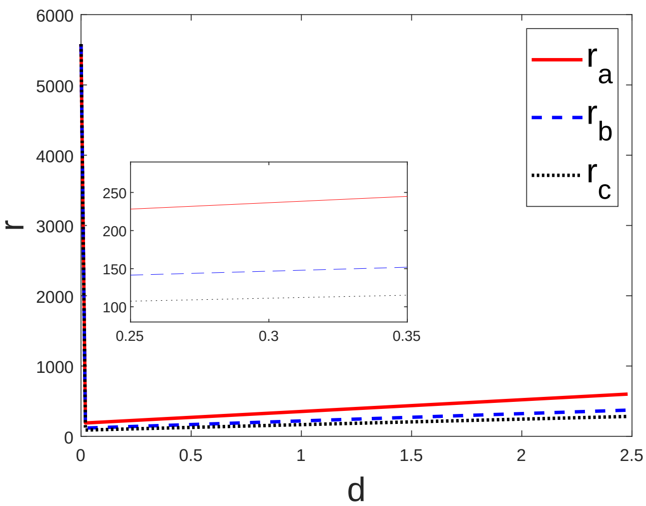

Fig. 10. The synchronization ability index changes with d

nized region. r_a, r_b and r_c represent the synchronization ability indexes of $G_c(c,m,k)(c=1,2,3)$ in the case of

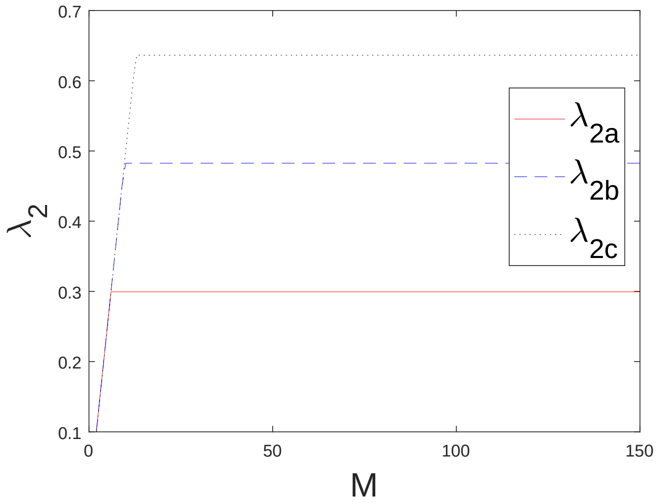

Fig. 11. The synchronization ability index changes with M

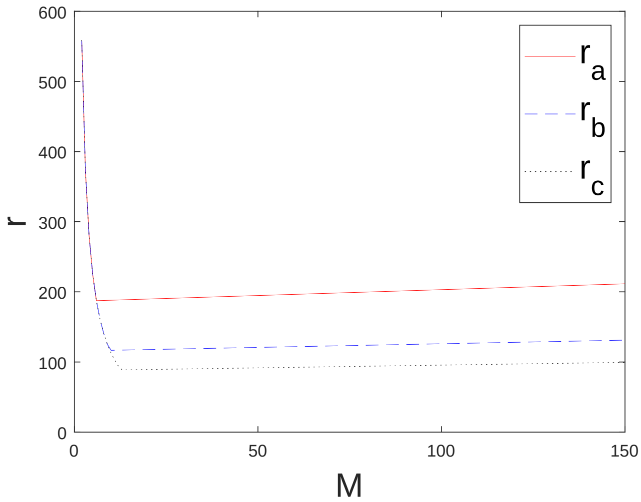

Fig. 12. The synchronization ability index changes with M

bounded synchronized region.

We take $k=7, a=2, d=0.05, M=50$, and increase m from 3 to 300 in Fig. 3 and Fig. 4. In the unbounded synchronized region, when $m<256(m<242, m<189)$, λ_{2a} rapidly decreases to 0.2251, λ_{2b} rapidly decreases to 0.4084, and λ_{2c} rapidly decreases to 0.5598. When $m>256(m>242, m>189)$, λ_{2a} , λ_{2b} and λ_{2c} remain unchanged with the increase of m. In the bounded synchronized region, r_a, r_b and r_c increase with the increase of m.

We take $m=10, a=2, d=0.005, M=50$, and increase k from 2 to 100 in Fig. 5 and Fig. 6. In the unbounded synchronized region, when $k<8(k<16, k<24)$, λ_{2a} , λ_{2b} and λ_{2c} remain unchanged at 0.2500. When $k>8(k>16, k>24)$, λ_{2a} rapidly decreases to 0.0270, λ_{2b} rapidly decreases to 0.0477, and λ_{2c} rapidly decreases to 0.0686. In the bounded synchronized region, r_a, r_b and r_c increase with the increase of k.

We take $m=10, k=7, d=0.005, M=50$, and increase a from 0.5 to 3 in Fig. 7 and Fig. 8. In the unbounded synchronized region, when $a<1.67(a<1.04, a<0.79)$, λ_{2a} , λ_{2b} and λ_{2c} slowly increase to 0.2500. When

$a > 1.67(a > 1.04, a > 0.79)$, λ_{2a}, λ_{2b} and λ_{2c} remain unchanged at 0.2500. In the bounded synchronized region, when $a < 1.67(a < 1.04, a < 0.79)$, r_a slowly decreases to 189.0116 , r_b slowly decreases to 116.6278, r_c slowly decreases to 89.0082. When $a > 1.67(a > 1.04, a > 0.79)$, r_a, r_b and r_c rapidly increase to 335.8270.

We take $m = 10, k = 7, M = 50, a = 2$, and increase d from 0.002 to 2.5 in Fig. 9 and Fig. 10. In the unbounded synchronized region, when $d < 0.006(d < 0.010, d < 0.013)$, λ_{2a} slowly increase to 0.2994, λ_{2b} slowly increase to 0.4826, λ_{2c} slowly increase to 0.6365. When $d > 0.006(d > 0.010, d > 0.013)$, λ_{2a}, λ_{2b} and λ_{2c} remain unchanged. In the bounded synchronized region, when $d < 0.006(d < 0.010, d < 0.013)$, r_a slowly decreases to 187.4375, r_b slowly decreases to 116.6269, r_c slowly decreases to 88.7136. When $d > 0.006(d > 0.010, d > 0.013)$, r_a slowly increases to 603.8856, r_b slowly increases to 374.5799, and r_c slowly increases to 284.0456.

We take $m = 10, k = 7, d = 0.05, a = 2$, and increase M from 2 to 150 in Fig. 11 and Fig. 12. In the unbounded synchronized region, when $M < 6(M < 10, M < 13)$, λ_{2a} slowly increase to 0.2994, λ_{2b} slowly increase to 0.4826, λ_{2c} slowly increase to 0.6365. When $M > 6(M > 10, M > 13)$, λ_{2a}, λ_{2b} and λ_{2c} remain unchanged. In the bounded synchronized region, when $M < 6(M < 10, M < 13)$, r_a slowly decreases to 187.4041, r_b slowly decreases to 116.6579, r_c slowly decreases to 88.8550. When $M > 6(M > 10, M > 13)$, r_a slowly increases to 211.4541, r_b slowly increases to 131.1613, and r_c slowly increases to 99.4602.

V. MAIN RESULTS

A. Result 1

Gao et al. obtains the synchronization ability indexes $\lambda_2^\star$ and $r^\star$ of star-composed networks [25], $\lambda_2^\star = min\{\frac{c+k+1-\sqrt{(c+k+1)^2-4c}}{2}a, Md\}$, $r^\star = \lambda_{max}^\star/\lambda_2^\star$, where $\lambda_{max} = \frac{m+k+2+\sqrt{(m+k+2)^2-4(m+1)}}{2}a + Md$. Although the number of network nodes in this paper are the same as that in the literature [25], the synchronization ability indexes are very different. In this paper, $\lambda_2 = min\{\frac{g_1+c+k+1-\sqrt{(g_1+c+k+1)^2-4(g_1+c)}}{2}a, Md\}$, $r = \lambda_{max}/\lambda_2$, where $g_1 = 4sin^2(\frac{\pi}{m+1-c})$, $\lambda_{max} = \frac{m+k+2+\sqrt{(m+k+2)^2-4(m+1)}}{2}a + Md$. From the properties of the function, we can deduce $\lambda_2 \geq \lambda_2^\star$. Because of $\lambda_{max} = \lambda_{max}^\star$, therefore $r \leq r^\star$. Whether the synchronized region is unbounded or bounded, the synchronization ability of this paper is better than that of star-composed networks [25].

B. Result 2

When the synchronized region is unbounded, the specific relationships among synchronization ability and parameters are as follows.

With the increase of m, $m < m^*$, λ_2 rapidly decreases, $m > m^*$, λ_2 remain unchanged, where $m^* = \frac{2\pi}{arccos(1-\frac{M^2d^2-Mdka-Mda}{2a(Md-a)}+\frac{c}{2})} + c - 1$. When $m < m^*$, the synchronization ability is negatively correlated with m. When $m > m^*$, the change of m will not affect the synchronization ability. The synchronization ability of networks is optimal at $m = c + 2$.

With the increase of k, $k < k^*$, λ_2 remain unchanged, $k > k^*$, λ_2 slowly decreases, where $k^* = \frac{ab}{Md} + \frac{Md}{a} - b - 1$. When $k < k^*$, the synchronization ability remain unchanged. When $k > k^*$, the synchronization ability is negatively correlated with k. The synchronization ability of networks is optimal at $k = 2$.

With the increase of $a(d, M)$, $a < a^*(d < d^*, M < M^*)$, λ_2 increases at first, $a > a^*(d > d^*, M > M^*)$, λ_2 remain unchanged, where $a^* = \frac{2Md}{b+k+1-\sqrt{(b+k+1)^2-4b}}$, $d^* = \frac{b+k+1-\sqrt{(b+k+1)^2-4b}}{2M}a$, $M^* = \frac{b+k+1-\sqrt{(b+k+1)^2-4b}}{2d}a(b = c + 4sin^2(\frac{\pi}{m+1-c}))$. When $a < a^*(d < d^*, M < M^*)$, the synchronization ability is positively correlated with $a(d, M)$. When $a > a^*(d > d^*, M > M^*)$, the change of $a(d, M)$ will not affect the synchronization ability. The synchronization ability of networks is optimal at $a = a^*, d = d^*, M = M^*$.

When the synchronized region is bounded, the specific relationships among synchronization ability and parameters are as follows.

With the increase of $m(k)$, r is increased, the synchronization ability is negatively correlated with $m(k)$. The synchronization ability of networks is optimal at $m = c + 2, k = 2$.

With the increase of $a(d, M)$, $a < a^*(d < d^*, M < M^*)$, r decreases at first, $a > a^*(d > d^*, M > M^*)$, r continues to increase. When $a < a^*(d < d^*, M < M^*)$, the synchronization ability is positively correlated with $a(d, M)$. When $a > a^*(d > d^*, M > M^*)$, the synchronization ability is negatively correlated with $a(d, M)$. The synchronization ability of networks is optimal at $a = a^*, d = d^*, M = M^*$.

Based on the above analysis, whether the synchronized region is unbounded or bounded, the synchronization ability of networks is optimal at $m = c + 2, k = 2, a = a^*, d = d^*, M = M^*$.

C. Result 3

Through the numerical simulation experiment and analysis in section IV, $\lambda_{2a} \leq \lambda_{2b} \leq \lambda_{2c}$, when the synchronized region is unbounded, the synchronization ability of the networks increases with the increase of central nodes. $r_c \leq r_b \leq r_a$, when the synchronized region is bounded, the synchronization ability of the networks also improves with the increase of central nodes.

VI. CONCLUSION

In this paper, a new multi-layer wheel network model is constructed on the basis of star-ring network. The MSF method is used to analyze the synchronization ability of the networks. Under the same initial conditions, the synchronization ability of the network model constructed in this paper is better than that in the literature [25]. We simulate the relationships among the synchronization ability and various parameters, such as the length of cycle m, the number of nodes k in path. Whether the synchronized region is unbounded or bounded, $m = c + 2, k = 2, a = a^*, d = d^*, M = M^*$, the synchronization ability of networks is optimal. We further consider the impact of the central node on the synchronization ability of the networks, whether the synchronized region is unbounded or bounded, the synchronization ability of the networks improves with the increase of central nodes, our conclusion provides an effective strategy for improving the synchronization ability of the networks.

REFERENCES

[1] S. Borgatti, A. Mehra, D. Brass, and G. Labianca, "Network analysis in the social sciences," *Science*, vol. 323, no. 5916, pp. 892-895, 2009.

[2] H. Guan, B. Yang, and H. Wang, "Multiple faults diagnosis of distribution network lines based on convolution neural network with fuzzy optimization," *IAENG International Journal of Computer Science*, vol. 47, no. 3, pp. 567-571, 2020.

[3] N. Li, X. Wu, J. Feng, and Y. Xu, "Fixed-time synchronization of coupled neural networks with discontinuous activation and mismatched parameters," *IEEE Trans Neural Netw Learn Syst*, vol. 32, pp. 2470-2482, 2021.

[4] Y. Yao, and H. Yao, "Finite-time Control of Complex Networked Systems with Structural Uncertainty and Network Induced Delay," *IAENG International Journal of Applied Mathematics*, vol. 51, no. 3, pp. 508-514, 2021.

[5] X. Qu, X. Li, and X. Cao, "Quantized Adaptive Bounded-H-infinity Tracking Control for a Class of Stochastic Nonaffine Nonlinear Systems," *IAENG International Journal of Applied Mathematics*, vol. 52, no.2, pp. 298-307, 2022.

[6] M. Aslam, C. Xue, M. Liu, K. Wang, and D. Cui, "Classification and Prediction of Gastric Cancer from Saliva Diagnosis using Artificial Neural Network," *Engineering Letters*, vol. 29, no. 1, pp. 10-24, 2021.

[7] S. Jafarizadeh, F. Tofigh, J. Lipman, and M. Abolhasan, "Optimizing synchronizability in networks of coupled systems," *Automatica*, vol. 112, pp. 108711, 2020.

[8] J. Gao, and Y. Chen, "Finite-time and Fixed-time Synchronization for Inertial Memristive Neural Networks with Time-varying Delay and Linear Coupling," *IAENG International Journal of Applied Mathematics*, vol. 52, no.3, pp. 534-540, 2022.

[9] K. Daley, K. Zhao, and I. Belykh, "Synchronizability of directed networks: The power of non-existent ties," *Chaos: An Interdisciplinary Journal of Nonlinear Science*, vol. 30, no. 4, pp. 043102, 2020.

[10] W. Du, "Adaptive Synchronization of Two Layers Coupled Network with Multi-weights and Time-varying Delay," *IAENG International Journal of Computer Science*, vol. 48, no. 4, pp. 1175-1181, 2021.

[11] J. Zhu, D. Huang, H. Jiang, J. Bian, and Z. Yu, "Synchronizability of multilayer variable coupling windmill-type networks," *Mathematics*, vol. 9, no. 21, pp. 2721, 2021.

[12] M. Chutani, B. Tadic, and N. Gupte, "Hysteresis and synchronization processes of Kuramoto oscillators on high-dimensional simplicial complexes with the competing simplex-encoded couplings," *Physical Review E*, vol. 104, pp. 034206, 2021.

[13] X. Wu, H. Men, J. Lu, J. Hu, and X. Han, "Analysis of the synchronizability of two-layer chain networks with two inter-layer edges," *Scientia Sinica informationis*, vol. 51, no. 11, pp. 1931-1945, 2021.

[14] X. Wang, A. Tejedor, Y. Wang, and Y. Moreno, "Unique superdiffusion induced by directionality in multiplex networks," *New Journal of Physics*, vol. 23, pp. 013016, 2021.

[15] H. Yan, J. Zhou, W. Li, J. Lu, and R. Fan, "Superdiffusion criteria on duplex networks," *Chaos*, vol. 31, pp. 073108, 2021.

[16] V. Leli, S. Osat, T. Tlyachev, D. Dylov, and J. Biamonte, " Deep learning super-diffusion in multiplex networks," *Journal of Physics: Complexity*, vol. 2, no. 3, pp. 035011, 2021.

[17] X. Wu, W. Wei, L. Tang, J. Lu, and J. L*ü*, "Coreness and h-index for weighted networks," *IEEE Transactions on Circuits and Systems*, vol. 66, pp. 3113-3122, 2019.

[18] J. Yang, J. Lu, Y. Wu, T. Li, and Y. Yang, "A Node Ranking Method Based on Local Structure Information in Complex Networks," *Engineering Letters*, vol. 30, no.1, pp. 161-167, 2022.

[19] H. Parastvand, A. Chapman, O. Bass, and S. Lachowicz, "The Impact of Graph Symmetry on the Number of Driver Nodes in Complex Networks," *Journal of the Franklin Institute*, vol. 358, no. 7, pp. 3919-3942, 2021.

[20] L. Tang, X. Wu, J. Lu, J. A. Lu, and R. M. D'Souza, "Master stability functions for complete, intra-layer, and inter-layer synchronization in multiplex networks of coupled Rossler oscillators," *Physical Review E*, vol. 99, no. 1, pp. 012304, 2019.

[21] J. Wei, X. Wu, J. Lu, and X. Wei, "Synchronizability of duplex regular networks," *Europhys Lett*, vol. 120, no. 2, pp. 20005, 2018.

[22] X. Wei, X. Wu, J. Lu, J. Wei, J. Zhao, and Y. Wang, "Synchronizability of two-layer correlation networks," *Chaos*, vol. 131, pp. 103124, 2021.

[23] F. Yang, Z. Jia, and Y. Deng, "Eigenvalue Spectrum and Synchronizability of Two Types of Double-Layer Star-Ring Networks with Hybrid Directional Coupling," *Discrete Dynamics in Nature and Society*, pp. 6623648, 2021.

[24] S. Barik, and G. Sahoo, "On the Laplacian spectra of some variants of corona," *Linear Algebra Its Appl.* vol. 512, pp. 32-47, 2017.

[25] H. Gao, J. Zhu, X. Li, and X. Chen, "Synchronizability of Multi-Layer-Coupled Star-Composed Networks," *Symmetry*, vol. 13, pp. 2224, 2021.